

Fluorapatite-Gelatine Nanocomposites: Induction of a Hierarchical Morphogenesis by Intrinsic Electric Dipole Fields — A General Principle in Biomineralization?

Paul Simon, Dirk Zahn, Hannes Lichte¹, and Rüdiger Kniep

The biomimetic system fluorapatite-gelatine bears strong resemblance to the bio-system hydroxyapatite-collagen which plays a decisive role in the human body as functional material in the form of bone [1] and teeth [2]. In both systems, the hierarchical and self-similar organization of nano-composite structures is of prominent relevance [3-6]. The morphogenesis of fluorapatite-gelatine nanocomposites features the essential advantage to reveal a concise sequence of growth developments, whereas bone and teeth are formed by a much more complex process on the basis of involvement of cell activities in a living system. Substitution of the rigid, non-soluble collagen by water-soluble gelatine (denatured collagen) takes advantage of a high mobility and accessibility and therewith, an enhanced reactivity of the functional groups of the biopolymer derivative.

Fluorapatite-gelatine nanocomposites (98 wt.-% apatite) are grown in buffered aqueous solutions of calcium, phosphate and fluoride ions, migrating into a gelatine-gel plug in a double diffusion cell [7-14]. Within a few days, so-called Liesegang bands are

formed consisting of the grown composite aggregates. Initial stages of growth comprise micrometer-sized, hexagonal prismatic composite seeds (marked violet in Fig. 1a). These species develop in subsequent growth stages to dumbbells states and complete their development as closed, notched spheres (Fig. 1a). The morphogenesis can be described as a fractal growth mechanism with a total of about 10 generations and a reduction factor of 0.7 in successive generations [8,11]. The presence of mineralized macromolecules in the fluorapatite-gelatine nanocomposites was already shown in former works [12,13]. The appearance of dislocations and a resulting superstructure pattern at the nanometer scale observed in transmission electron microscopy (TEM) high-resolution micrographs indicate the presence of incorporated gelatine macromolecules running parallel [001] within the composite seed. The superstructure is visualized in the Fast Fourier Transform (FFT) of the high-resolution images in form of diffuse streaks around the primary beam with a periodicity of about 5 nm and multiples of this value (Fig. 1b) [12]. The diffuse streaks are run-

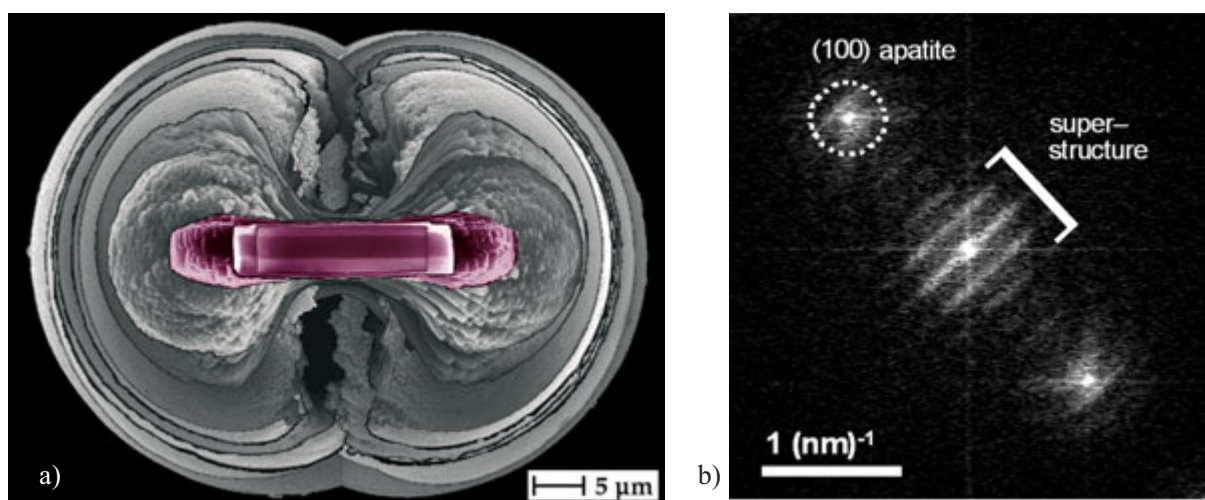


Fig 1: (a) Superposition of growth stages of fractal fluorapatite-gelatine nanocomposite aggregates (scanning electron microscopy images). The morphogenesis starts with an elongated hexagonal prismatic seed, which develops via out-growth areas at both ends (central violet area). Subsequently, the aggregate forms dumbbell shaped structures, and finally ends up with a closed (notched) sphere. (b) Superstructure of the central composite seed caused by mineralized gelatine triple helices observed in the FFT of TEM high-resolution micrographs as diffuse streaks around the primary beam with a periodicity of about 5 nm and multiples of this value. For further details see text.

ning parallel to the (100) reflections of apatite, thus showing the ordered intergrowth of the organic and the inorganic components.

Already in 1999, the possible influence of intrinsic electric fields on the fractal morphogenesis of fluorapatite-gelatine nanocomposite aggregates was discussed [8,11]. Model calculations of the electric fields around the seed- and the dumbbell-states were carried out, whereas detailed knowledge of the inner structure of these growth stages was not available at that time [8]. A change of morphology could be achieved by applying an external electric field ($E = 5000 \text{ V}/1.4 \text{ cm DC}$) [8]. Generally, the growth rate was lowered and rounded upgrowth regions were observed instead of prismatic splitting of the seed without the external field. The influence of electric fields on other relevant biological systems could be also proved. In 1996, *Yamashita et al.* demonstrated that the growth rate of bone-like layers can be affected by surface polarization of hydroxyapatite (HAp) or ferroelectric BaTiO_3 substrates by an applied external electric field [15]. This observation has a large impact for bone implantation because there is lively interest to induce apatite mineralization on synthetic substrates and to stimulate bone adhesion on the implant [16]. Alongside, the piezoelectric effect of bone was used by applying external electric

fields in order to improve the bone healing processes. Inside of bone and tendon, collagen fibrils are arranged parallel to their long axes. The triple-helical molecules exhibit point group 3 and can be both piezo- and pyroelectric. The generation of electric fields caused by mechanical stress is attributed to the piezoelectric effect of collagen, whereas pyroelectricity proved to be low [17]. Fluorapatite features the centrosymmetric crystal class 6/m, therefore neither piezo- nor pyroelectricity can be considered. However, *Yamashita et al.* showed, that in the case of hydroxyapatite, polarizability is evoked by a reorientation of the dipole moments of OH^- . In this way, accelerated crystal growth was observed on polarized HAp surfaces [15].

The influence of an electric field on the mineralization process of polystyrenesulfonate (PSS) by CaCO_3 was observed by *Wang et al* [18]. Positive polarization of the (001) crystal surface of CaCO_3 led to selective adsorption of negatively charged PSS molecules. Formation of composite nanocrystal blocks was followed by their aggregation, thus forming mesocrystals. Theoretical calculations showed that such non-spherical charged objects in an electrolyte solution cause an anisotropic electric potential, giving rise to mutual alignment. Recently, single-molecule manipulation by means of scanning

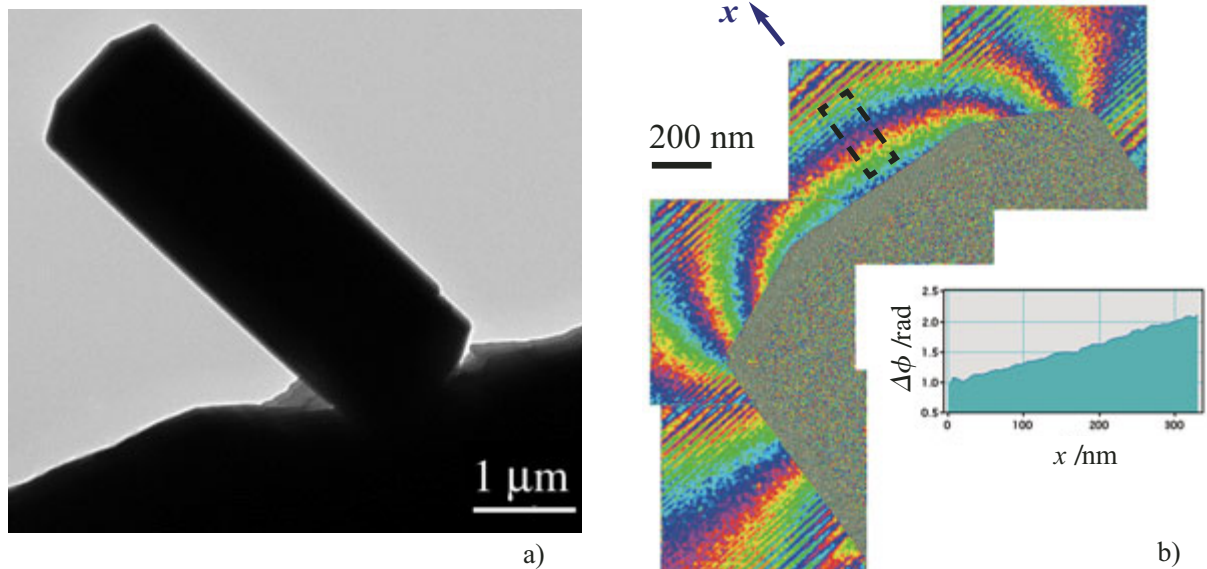


Fig. 2: (a) Hexagonal prismatic fluoroapatite-gelatine nanocomposite seed; conventional TEM micrograph. (b) Retrieved phase image of an electron hologram (8 times boosted, composed of 4 single images) exhibits the electric potential distribution around a seed. Color code denotes a phase shift of 2π from green to green. Fresnel fringes of the interferograms appear as striation patterns at the corners of the phase images. The observed projected potential corresponds to a mesoscopic dipole. The phase profile is depicted from the rectangle with dotted borderline at the basal plane and reveals a phase increase of about 1 rad per 300 nm (inset, b).

tunneling microscopy on biopolymers was reported by using electrical fields and conductivity switching. The helical structure and molecule length of a peptide bundle could be varied by application of an external field due to the interaction of the field with the large dipole moment of the helix [19].

The summarized results discussed in the preceding part and our experimental work on the fluorapatite-gelatin nanocomposites encouraged us to investigate the influence of intrinsic electric fields on the morphogenesis and morphology of these aggregates in more detail. We focused our efforts on the composite seed since it represents the initial and thus, the fundamental growth step during the morphogenesis. The nanocomposite seed itself already consists of a self-similar and hierarchical inner nano-structure [13]. Our actual TEM investigations show that mineralized triple helices form a 3D-framework and that these protein macromolecules within the composite seed are in parallel orientation with the long axis of the composite seed which is the crystallographic c -axis of the highly mosaic-controlled apatite specimen [12,13,20]. We assume that the triple helices exhibit opposite charges at their ends, and that by adding up all these microscopic dipoles a macroscopic electric dipole of the composite system is formed. This could have an important or even a decisive influence on further growth steps and thus the fractal morphogenesis.

Here, we chose electron holography in order to image the electric fields. This method allows to record both, phase and amplitude of the image wave. The phase holds information which is lost in the amplitude images (corresponding to conventional images). The electrical potential distribution integrated along the beam direction produces a phase shift of the incident electron wave which is registered by means of an interferogram. Thus, electron holography offers the unique opportunity to visualize, e.g., electric or magnetic micro- and nanofields [21,22].

In Fig. 2a, a conventional TEM micrograph of a hexagonal prismatic seed with the typical aspect ratio close to 3:1 is shown. Only the silhouette of the seed is visible, whereas the phase image (8 times boosted) clearly shows the electric potential distribution around the seed (Fig. 2b). The observed projected potential strongly resembles a macroscopic dipole. The phase profile is taken from the area marked by a dotted borderline at the base

plane and shows a phase increase of about 1 rad per 300 nm (Fig. 2b, right below). This finding corresponds to about 0.13 times the polarization observed inside BaTiO₃ ($P = 0.26 \text{ C/m}^2$, $\epsilon_r \sim 1700$).

Subsequently, we performed calculations in order to check our assumption that the macro dipole is composed of an assembly of elementary dipoles at the nanometer scale. The model is based on the assumption of all dipoles being aligned parallel to the c -axis of the composite seed (Fig. 3a, arrows

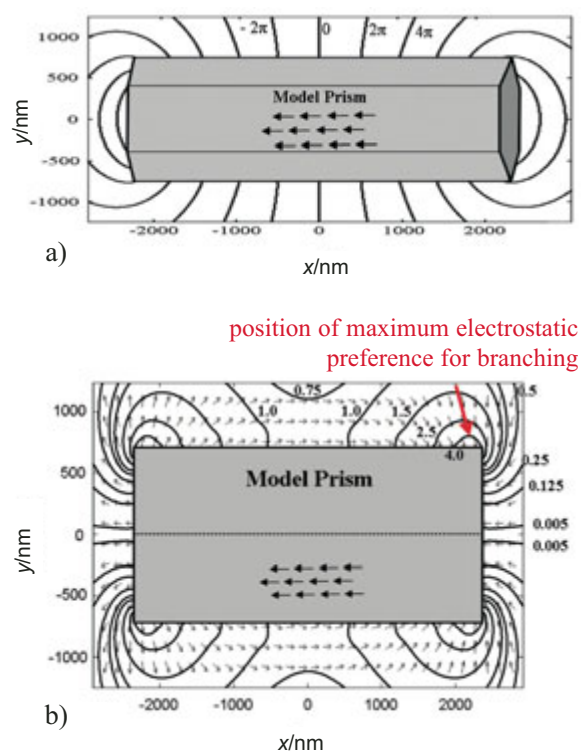


Fig. 3: (a) Simulation of the phase image around a nanocomposite seed based on an ideal arrangement of nano-dipoles. The model is constructed of triple helices in parallel orientation along [001] within the seed. Triple helices represent dipoles and are depicted as arrows; schematic representation. For further details see text. The contour plot of the phase shift shows a good qualitative agreement with the electron holographic experimental data. (b) Calculation of preferred orientation of the triple helices attaching from the gel and energy isolines around a composite seed in aqueous solution ($\epsilon_r \sim 78$). The energy isolines (kJ mol^{-1}) indicate where and "how" neighboring macromolecules from the gel are attached to the seed. Largest divergence is produced at the corners, especially at the prism faces near the basal planes of the seed (red arrow). At these positions, there is also strongest tendency for triple helices from the gel to adopt a different orientation with respect to the hexagonal c -axis and thus to give evidence for branching at both ends of the seed (beginning of fractal growth).

within the seed). Thereby, we adopt the hypothesis that each triple helical gelatine molecule shows an idealized protonation state, i.e., all the N-termini are completely protonated and all the C-termini are deprotonated. The lengths of the fiber proteins and their vertical spacings were chosen according to TEM micrographs [12,13]. Contour plots of the phase shift calculated on the base of this structural model are shown in Fig. 3a, in which each isoline corresponds to a phase shift of 2π . The comparison with experimental data gives a qualitative and direct agreement to the computer model. Therefore, in principle, the assumption of a nano-dipole model seems to be reasonable. However, a quantitative analysis yields that the phase shift of the model calculations compared with measured values is overestimated by a factor of 8. A possible reason for this could be a deviation from idealized protonation/deprotonation states of the $-\text{NH}_3^+$ and $-\text{COO}^-$ functional groups. Another source of error could be given by the estimated values for the length of the collagen molecules and their lateral spacing among each other. Finally, some triple helices may adopt an antiparallel orientation with respect to each other and thus, some electric dipoles may be neutralized. However, these discrepancies between observed and calculated patterns do not change the qualita-

tive truth of the character of the contour plot. A quantitative agreement can be achieved by a global scaling parameter of $1/8$. This factor comprehends microscopic aberrations by averaging and thus, provides a model with mesoscopic resolution which is quantitatively correct.

Assuming an effective dipole moment of $1/8e \times 300 \text{ nm}$ for every triple helix, we constructed an energy profile which displays the local preferred position and orientation of triple helices coupling out of the aqueous gel onto the surface of the seed. Thereby, the dielectric effect of the medium $\epsilon_r = 78$ (water) was assessed. Certainly, this value features an upper limit since the dielectricity number of apatite of about 8 is significantly lower. Arrows in Fig. 3b exhibit the energetically most preferred positions and orientations, exclusively based on Coulomb interactions of the dipole model. The energy difference concerning the orientation and the alignment within the seed is given by means of isopotential lines. Most of the triple helices in solution (in the gel) prefer a different orientation than those within the seed. This tendency is mostly pronounced at the prism faces in the vicinity of the basal plane. The energy difference between the orientation parallel $[001]$ and the preferred (new) arrangement amounts to at least 4 kJ mol^{-1} .

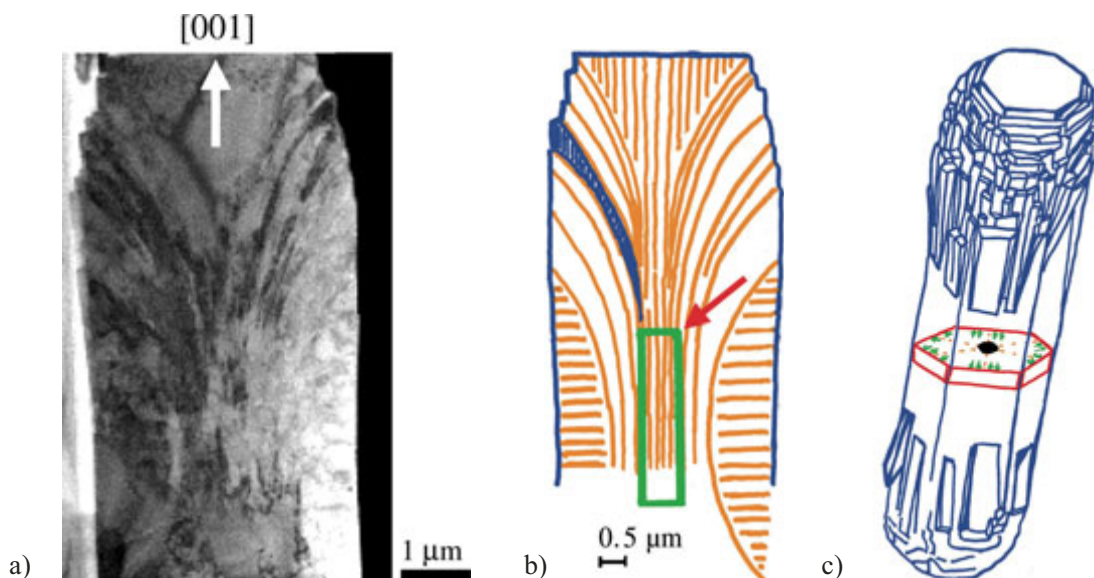


Fig. 4: (a) TEM overview image of a “nearly splitting” seed; cut parallel $[001]$ prepared by means of focused ion beam (FIB) technique. The outgrowth-area for the next (1^{st}) generation is clearly indicated by the contour-steps near the basal plane. (b) Schematic sketch of (a) showing the hierarchical arrangement of gelatine triple helices and fibrils (orange) within a mature seed specimen before splitting. Central seed: green bordered area. At the corners of the central seed branching begins. The area with highest tendency for branching (see Fig. 3b) is marked with a red arrow. A schematic sketch (3D-representation) for the growth state of the nanocomposite under discussion is shown in (c).

During the formation of the composite the surrounding solvent (water) will be replaced by apatite and hence, the dielectric effect is decreased by a factor of about 1/10 and the energy difference can be estimated up to 40 kJ mol⁻¹.

Locations showing highest probability of electrostatic orientational deviation coincide with the experimentally observed branching positions of a seed. The process of branching is already clearly recognized in the mature growth state of the seed. In TEM micrographs of samples thinned by focused ion beam technique (FIB) (Fig. 4a), rolling arcs are observed which start at the initial seed (Fig. 4b, central green rectangle) and trend outside, whereas at the basal plane the composite seed continues to grow in direction of the hexagonal *c*-axis.

Our investigations support a correlation between intrinsic fields and the self organized growth of the bio-composite system fluorapatite-gelatine. These fields are caused by a parallel orientation of triple helical protein fibres of gelatine and produce, in the case of fluorapatite-gelatine seeds, a mesoscopic dipole field. The model calculations show that branching at the ends of the elongated seed is caused by an energetically favored orientation of triple helices significantly off the hexagonal *c*-axis direction. At this point a next higher level of hierarchy occurs by oriented bundling of gelatine macromolecules and formation of micro-fibrils which stretch out of the volume with bent patterns (Fig. 4). Thus, the dipole field influences the further growth development of the seed and in this way: it monitors the fractal morphogenesis of the composite aggregate. Our results enable a deeper understanding of the growth of biological composites such as bone and teeth and open up new perspectives to influence or monitor this process by means of electrical fields. Further work will comprise imaging and simulation of the electric field of the mature growth stages and of isolated triple helical fiber proteins in order to understand the influence of electric fields onto the fractal pattern formation.

We would like to thank Dr. W. Carrillo-Cabrera and Dr. P. Formanek for helpful discussions and experimental support.

References

- [1] *F. Bronner, M. Farach-Carson* (Eds.), Bone Formation, Springer publisher, 2003.
- [2] *M. F. Teaford, M. M. Smith, M. W. J. Ferguson* (Eds.) Development, Function and Evolution of Teeth, Cambridge University Press, 2000.
- [3] *A. R. Matthew, I. Jasiuk, J. Taylor, J. Rubin, T. Ganey and R. P. Apkarian*, Bone **33** (2003) 270.
- [4] *H. S. Gupta, W. Wagermaier, G. A. Zickler, D.R.B Aroush, S. S. Funari, P. Roschger, H. D. Wagner and P. Fratzl*, Nano Lett. **5** (10) (2005) 2108.
- [5] *R. Tang, L. Wang, C. A. Orme, T. Bonstein, P. J. Bush and G. H. Nancollas*, Angew. Chem. Int. Ed. **43** (2004) 26971.
- [6] *A. Veis*, Science **307** (2004) 419-420.
- [7] *R. Kniep and S. Busch*, Angew. Chem. **108** (1996) 2787; Angew. Chem. Int. Ed. Engl. **35** (1996) 2624.
- [8] *S. Busch, H. Dolhaine, A. DuChesne, S. Heinz, O. Hochrein, F. Laeri, O. Podebrand, U. Vietze, T. Weiland and R. Kniep*, Eur. J. Inorg. Chem. **10** (1999) 1643-1653.
- [9] *S. Busch, U. Schwarz and R. Kniep*, Chem. Mater. **13** (2001) 3260.
- [10] *S. Busch, U. Schwarz and R. Kniep*, Adv. Funct. Mater. **13** (2003) 189.
- [11] *R. Kniep* in Facetten einer Wissenschaft (Eds. *A. Müller, H. J. Quadbeck-Seeger and E. Diemann*), Wiley-VCH, Weinheim, 2004.
- [12] *P. Simon, W. Carrillo-Cabrera, P. Formanek, C. Göbel, D. Geiger, R. Ramlau, H. Tlatlik, J. Buder and R. Kniep*, J. Mater. Chem. **14** (2004) 2218.
- [13] *P. Simon, U. Schwarz and R. Kniep*, J. Mater. Chem. **15** (47) (2005) 4992.
- [14] *H. Tlatlik, P. Simon, A. Kawska, D. Zahn and R. Kniep*, Angew. Chem. Int. Ed., in press.
- [15] *K. Yamashita, N. Oikawa and T. Umegaki*, Chem. Mater., **8** (1996) 2697.
- [16] *P. Calvert and S. Mann*, Nature **386** (1997) 127.
- [17] *S. B. Lang*, Nature **212** (1966) 704.
- [18] *H. Cölfen and M. Antonietti*, Angew. Chem. **117** (2005) 5714-5730; Angew. Chem. Int. Ed. Engl. **44** (2005) 5576.
- [19] *K. Kitagawa, T. Morita and S. Kimura*, Angew. Chem. Int. Ed. Engl. **117** (2005) 6488.
- [20] *P. Simon, H. Lichte, A. Valera, W. Carrillo-Cabrera, D. Mönter and W. Reschetilowski, Z. Allg. Anorg. Chem.* **631** (2005) 983.
- [21] *H. Lichte and M. Lehmann* in Advances in Imaging and Electron Physics, Electron Holography: A powerful tool for analysis of nanostructures, Elsevier Science (USA) **123** (2002) 225.
- [22] *H. Lichte, M. Reibold, K. Brand and M. Lehmann*, Ultramicroscopy **93** (2002) 199.

¹ Dresden University of Technology, Dresden, Germany